Birth Defects Research (Part C) 81:320–328 (2007)

REVIEW

Developmental Biology and Tissue Engineering

Francoise Marga, Adrian Neagu, Ioan Kosztin, and Gabor Forgacs*

Morphogenesis implies the controlled spatial organization of cells that gives rise to tissues and organs in early embryonic development. While morphogenesis is under strict genetic control, the formation of specialized biological structures of specific shape hinges on physical processes. Tissue engineering (TE) aims at reproducing morphogenesis in the laboratory, i.e., in vitro, to fabricate replacement organs for regenerative medicine. The classical approach to generate tissues/organs is by seeding and expanding cells in appropriately shaped biocompatible scaffolds, in the hope that the maturation process will result in the desired structure. To accomplish this goal more naturally and efficiently, we set up and implemented a novel TE method that is based on principles of developmental biology and employs bioprinting, the automated delivery of cellular composites into a three-dimensional (3D) biocompatible environment. The novel technology relies on the concept of tissue liquidity according to which multicellular aggregates composed of adhesive and motile cells behave in analogy with liquids: in particular, they fuse. We emphasize the major role played by tissue fusion in the embryo and explain how the parameters (surface tension, viscosity) that govern tissue fusion can be used both experimentally and theoretically to control and simulate the self-assembly of cellular spheroids into 3D living structures. The experimentally observed postprinting shape evolution of tube- and sheet-like constructs is presented. Computer simulations, based on a liquid model, support the idea that tissue liquidity may provide a mechanism for in vitro organ building. **Birth Defects Research (Part C) 81:320–328, 2007.** © 2008 Wiley-Liss, Inc.

INTRODUCTION

Tissue engineering (TE) is a relatively young field that aims at repairing, regenerating, or replacing damaged tissues with cellularized constructs grown in the laboratory (Langer and Vacanti, 1993; Vacanti and Langer, 1999). The arsenal of TE comprises those of cell biology, needed for finding a suitable cell source and for assuring conditions for cell growth, those of biomaterial chemistry, needed for preparing biocompatible support for anchorage dependent cells, and those of physiology, needed for maintaining a biomimetic, organ-specific environment in vitro (Vunjak-Novakovic, 2003). The promise of solving the problem of transplantable organ shortage is only one of the engines that drive TE research. Several laboratories and biotechnology companies have already developed organ modules that are used for tissue repair and regeneration. Moreover, functional subunits of human organs are viewed as a viable alternative for animal testing of new drugs (Griffith and Naughton, 2002).

As cells divide, differentiate, and organize into tissues and organs during embryonic development, they produce a tissue-specific mixture of interconnected protein filaments, the extracellular matrix (ECM). Besides offering a three-dimensional (3D) support for cells, the ECM is also involved in cell signaling (Mooney et al., 1992). Cell-ECM interactions play a crucial role in the function and structural integrity of the tissue. Instead of attempting to reproduce the very complex composition of ECM in vitro, TE aims at fabricating supportive scaffolds and identifying culture conditions that promote ECM production by cells. The basic tool in this endeavor is a bioreactor that allows for the controlled conditioning of the engineered construct (Vunjak-Novakovic, 2003). As the field of TE evolved, comparative studies between bioreactors have pointed to temperature control, gas exchange, mass transfer, shear stress, and other mechanical stimuli as essential factors of development and maturation. Because of differences between tissues, a ''one-size-fits-all'' bioreactor does not presently exist,

Francoise Marga and **Ioan Kosztin** are from the Department of Physics and Astronomy, University of Missouri–Columbia, Columbia, Missouri.
Adrian Neagu is from the Department of Physics and Astronomy, University of Missouri–Columbia, Columbia, Missouri and from the Victor Babeş University of Medicine and Pharmacy Timisoara, Timisoara, Romania.
Gabor Forgacs is from the Department of Physics and Astronomy and Department of Biological Sciences, University of Missouri–Columbia, Columbia, Missouri.

Grant sponsor: National Science Foundation; Grant number: FIBR-0526854; Grant sponsor: Romanian National Research Development and Innovation Program; Grant number: CEEX 11/2005 (to A.N.).

*Correspondence to: Gabor Forgacs, Department of Physics and Astronomy and Department of Biological Sciences, University of Missouri–Columbia, Columbia, MO 65211. E-mail: forgacsg@missouri.edu

Published online in Wiley InterScience (www.interscience.wiley.com). DOI: 10.1002/bdrc.20109

and a plethora of concepts and bioreactor designs have been created (Martin and Vermette, 2005; Chen, 2006).

Here, we review a recently developed TE method, that in many aspects differs from the more traditional techniques. It combines principles of developmental biology with novel engineering approaches to deliver biological materials into a 3D environment. Importantly, it is scaffold-free: biological structure formation primarily relies on the self-organizing properties of cells and tissues, not on external factors. Specifically, the method operates with multicellular spherical aggregates and utilizes them as bio-ink particles. These are delivered into the bio-paper, a cell specific environment by a special bioprinter that controls both the spatial and temporal aspects of the process. Biological structures form during the postprinting fusion of bio-ink particles as predicted by the amply demonstrated notion of tissue liquidity.

TISSUE LIQUIDITY

The differential adhesion hypothesis (DAH) (Steinberg, 1963) is a concept that explains morphogenesis on the basis of differences in the cell adhesion apparatus of different cell types. According to DAH, early morphogenesis is a self-assembly process (Whitesides and Boncheva, 2002): spontaneous structure formation by mobile and interacting building blocks (i.e., cells) (Steinberg, 1970; Gonzalez-Reyes and St Johnston, 1998; Foty and Steinberg, 2005; Perez-Pomares and Foty, 2006).

DAH is consistent with the view that, on a time scale of hours, embryonic tissues behave like highly viscous, incompressible liquids (Steinberg and Poole, 1982). The range of liquid-like behaviors comprise the rounding-up of initially irregular tissue fragments (in the absence of external forces), the fusion of two or more contiguous tissue fragments (Gordon et al., 1972), the engulfment of one tissue type by another via spreading (Foty et al., 1994), and the sorting of cell types in heterotypic mixtures (Technau and Holstein, 1992; Foty et al., 1994). Each of these phenomena has its classical liquid analogue. A liquid droplet assumes a spherical shape because of the mutual attraction of the constituent molecules; these take advantage of their mobility to seek positions that maximize their total binding energy and, thereby, minimize the surface area. Randomly intermixed molecules of immiscible liquids phase separate: the more cohesive liquid surrounds the less cohesive one. For example, mixing oil and water results in the latter being surrounded by the former. A similar arrangement results also by engulfment, when two droplets of different, immiscible liquids are put in contact.

Liquids can be characterized by surface or interfacial tension (γ) and viscosity (η). Analogous quantities have been determined for embryonic tissues using experimental techniques developed for liquids (Gordon et al., 1972; Foty et al., 1994, 1996; Forgacs et al., 1998). Apparent tissue surface tension was measured for several embryonic cell types, and the values were used to predict their mutual sorting behavior (Foty et al., 1996). The DAH provides the molecular basis for tissue surface tension by relating it to the strength of cell adhesion. Recent experiments (Foty and Steinberg, 2005) confirmed the theoretical prediction that tissue surface tension is proportional to the surface density of cell adhesion molecules (CAMs) (Forgacs et al., 1998). The implications of DAH have also been confirmed in vivo (Godt and Tepass, 1998; Gonzalez-Reyes and St Johnston, 1998; Hayashi and Carthew, 2004; Lecuit and Lenne, 2007) and by computer simulations (Glazier and Graner, 1993).

A particular phenomenon that may be understood in light of the DAH, is the ubiquitous morphogenetic process of tissue fusion that produced some of the evolutionary milestones in development (Perez-Pomares and Foty, 2006). An early manifestation of tissue fusion is the regeneration of individuals of the most basal metazoan lineages (e.g., porifera, cnidaria) by blending of small cut fragments (Wilson, 1907; Papenfuss, 1934). The continuity between the mouth, the digestive tract (with the pseudocoelom), and anus (that developed with the appearance of the nematodes) was established through the fusion of the pharynx and the oral cavity (Heid et al., 2001). The epiboly of the *Caenorhabditis elegans* hypodermis led to a fusion process known as the ventral enclosure (Williams-Masson et al., 1997). The appearance of the coelom, a true body cavity in the mollusks, was a major advance in animal body architecture. In addition to providing a hydrostatic skeleton, it made the development of a closed circulatory system possible (Munoz-Chapuli et al., 2005) and supplied a fluid-filled cavity in which organs could be suspended (Perez-Pomares and Munoz-Chapuli, 2002). Coelom formation has been scarcely studied, but observations on vertebrates reveal that tissue fusion is involved (Callebaut et al., 2004): small vesicles initially appear in the mesoderm along the anterior-posterior axis of the chicken embryo, then enlarge and fuse to form the coelomic cavity (Callebaut et al., 2004). The formation of a central nervous system in vertebrates and the four-chambered heart were yet other evolutionary steps that required tissue fusion. During neurulation, the neural plate creases inward, and the neural groove gradually deepens as the neural folds become elevated. Ultimately the edges come in contact and the folds fuse to convert the groove into the closed neural tube (Colas and Schoenwolf, 2001). In early heart development, it is the fusion of the atrioventricular cushions that leads to septation, the process during which the primitive heart tube transforms into a four-chambered organ with atria and ventricles (Wessels and Sedmera, 2003).

The above examples illustrate the important role of tissue fusion in early development. Our interest in

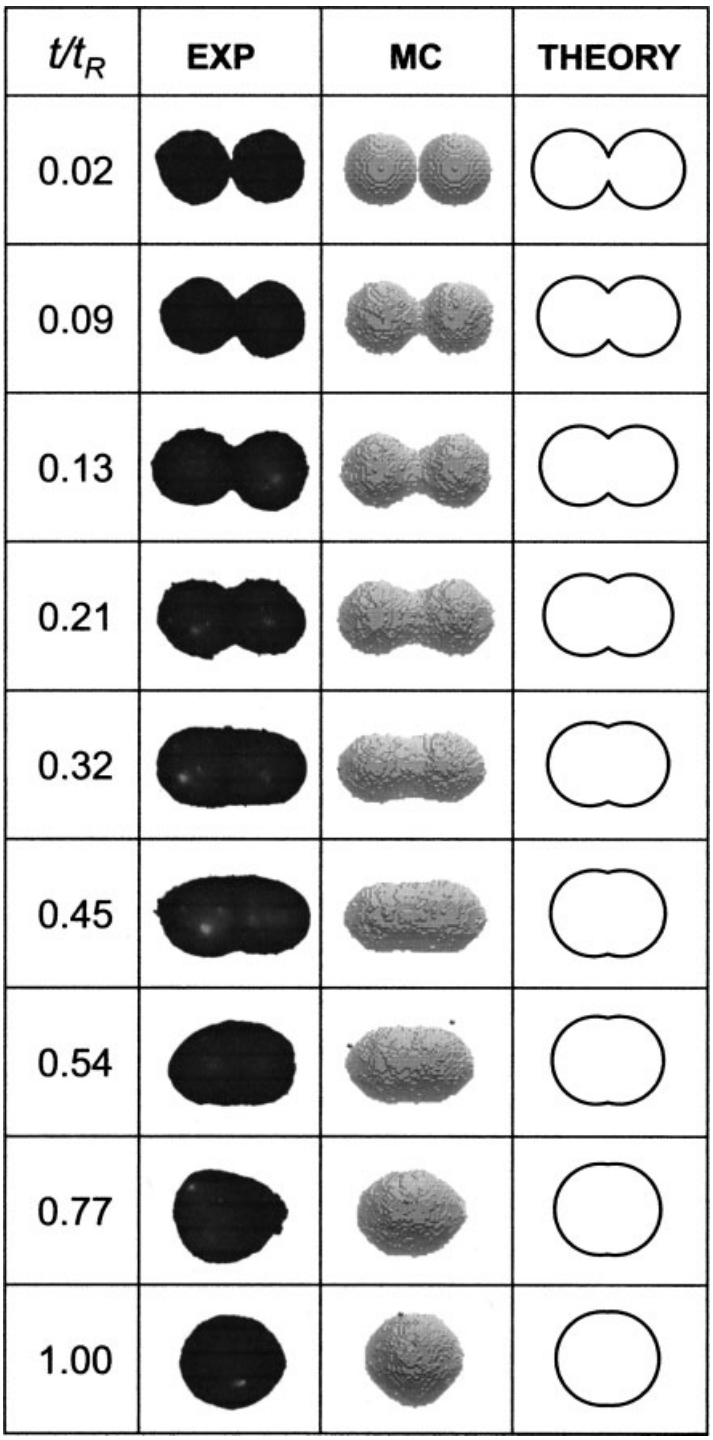

Figure 1. Snapshots of the fusion of spherical cell aggregates (500 μm in diameter) obtained from experiment, Monte Carlo (MC) simulations (with $\gamma_{12} = 0.5E_T$; see section "Computer Simulations of Postprinting Tissue Remodeling" for details), and theoretical modeling. The snapshots of the experimental (second column) and theoretical (fourth column) evolution were taken at times indicated in the first column (expressed in terms of the rounding, or total fusion time t_R). In the 3D column the snapshots were taken after 0, 3, 12, 50, 150, 300, 500, 800, and 1200 MCS.

developing a novel TE approach, based on directed self-assembly of cellular spheroids into 3D constructs of controlled shape and composition, motivated a thorough study of tissue fusion both experimentally, computationally, and theoretically (Flenner et al., 2007).

Experimentally, we prepared spherical aggregates (see below) and observed that upon contact they fused into a single sphere. Snapshots of successive stages of fusion are shown in Figure 1. To quantify the process, we followed the time evolution of the interfacial area of contact between the fusing tissue droplets and compared it with the similar process in true liquids. We found that not only the final equilibrium state but also the approach to it during the fusion of two spherical cell aggregates is liquid-like. For this we employed the theory of liquids to derive the shape of the interfacial contact area (Fig. 1). In particular, we established that the time scale, τ_0, that characterizes the fusion of the two highly viscous spherical droplets is given by $\tau_0 = \eta R_0/\gamma$, where η and γ are the viscosity and surface tension of the liquid and R_0 is the radius of the original droplets (as predicted by Frenkel, 1945). We were also able to express the total fusion (or rounding) time, $t_R \approx 3.5\tau_0$, where t_R is defined as the time when $r(t)$, the instantaneous radius of the circular interfacial region of the fusing aggregates, is $r(t_R) \approx 0.9R_f = 0.9(2^{1/3}R_0)$. Here R_f is the radius of the final (fused) single sphere, which is related to R_0 by the conservation of volume (Flenner et al., 2007). Our experimental results on the progression of cellular spheroids are in agreement with those obtained by the theoretical analysis of the fusion of true liquid drops (Flenner et al., 2007), and the measured value of τ_0 is compatible with the apparent tissue surface tension and viscosity measured by independent methods earlier (Forgacs et al., 1998).

DEVELOPMENTAL BIOLOGY–BASED TE

During early development, organs acquire their shape by complex, genetically orchestrated patterning, which is brought about by physical mechanisms. Novel TE approaches attempt to mimic natural morphogenesis by relying on

the capacity of cells to organize into tissues and eventually organs. A recent approach pursued in our laboratory employs aggregates of different cell types and relies on their self-assembly to produce functional organoids. As shown by proof-of-concept experiments (Jakab et al., 2004), this program can be realized by delivering spherical multicellular aggregates (bio-ink droplets) of definite composition into a supportive hydrogel (bio-paper) by bioprinting, an automated delivery process with a computer-controlled device.

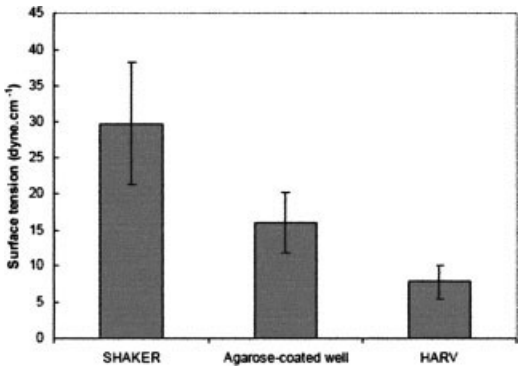

Figure 2. Comparison of the tissue surface tension of aggregates incubated on rotary shaker, agarose-coated well, and HARV. Error bars indicate SDs calculated on the basis of at least 12 compressions by condition.

Preprocessing: The Bio-Ink and the Bio-Paper

The bio-ink

Multicellular spheroids can be prepared from a single cell type or from a mixture of several cell types. The formation of spherical aggregates depends on cell-cell interactions, which may be direct, mediated by CAMs such as cadherins, or indirect, mediated by integrins—transmembrane proteins responsible for cell–ECM interactions. Several methods have been developed to produce the bio-ink from single-cell suspensions of trypsinized monolayer cultures. We briefly describe three of them.

In the hanging drop method, a drop of cell suspension is deposited on the cover of a Petri dish. Upon inversion of the cover, the droplet is held in place by the surface tension of the cell culture medium. Due to gravity, cells descend and accumulate at the bottom of the drop and associate to form a spheroid. The strength of cell–cell interactions determines the speed of aggregation, as well as the cohesiveness of the bio-ink droplet, while the density of the cell suspension controls the size of the aggregate. In another method, the cell suspension is centrifuged and the resulting sheet-like pellet that forms along the wall of the centrifuge tube is cut into small cubes of desired size, which upon incubation rapidly round into spheres. In the third method, the pellet obtained by centrifugation is transferred into capillary micropipettes. After a short incubation, a firm cellular ''sausage'' forms. Upon extrusion from the micropipette, the sausage-cylinder is cut into pieces of equal length and diameter, which subsequently round into spheres. (For further details see Hegedus et al. (2006)).

The biophysical properties of the aggregate depend not only on the cell type of which it is composed (Forgacs et al., 1998), but also on the method of incubation used during the rounding-up phase. Results in Figure 2, in particular, show how tissue surface tension (measured with a special-purpose tensiometer [Foty et al., 1994; Forgacs et al., 1998]) is affected when rounding takes place in a gyratory shaker, on an agarose-coated plate or in a high aspect ratio vessel (HARV) bioreactor (Prewett et al., 1993). This finding has important implications for our bioprinting efforts that rely on tissue liquidity, since the value of surface tension controls the rate of fusion of bio-ink particles. Thus, bio-ink preparation offers a possibility to control postprinting self-assembly of cells into tissue constructs.

For bioprinting, the spherical bio-ink droplets (multicellular aggregates) are packaged in cartridges (glass micropipettes of appropriate diameter), which are preserved in cell culture medium in the incubator until use (Jakab et al., 2006). The use of cellular spheroids as building blocks of tissues proved successful in recent cardiac TE experiments, which employed cardiomyocyte spheroids derived from embryonic stem cells (Wang et al., 2006).

The bio-paper

The strategy in TE is to use porous scaffolds (Hollister, 2005) or highly hydrated natural (Prestwich, 2007) or synthetic (Silva et al., 2004) polymers to sustain the attachment and the growth of the cells. Of these three materials, due to their high water content (up to 99%), hydrogels are the most biofriendly. They have been extensively used in bioengineering as drug delivery systems (Hubbell, 1996), wound dressing materials (Lay Flurrie, 2004), and support scaffolds for TE purposes (Lee and Mooney, 2001). Isolated ECM components, such as collagen, have also been used as bio-paper (Jakab et al., 2004). Recent advances in polymer chemistry however bear the promise of more versatile hydrogels. The Center for Therapeutic Biomaterials (CTB) at the University of Utah has developed synthetic ECM-like hydrogels based on co-cross-linked gelatin and hyaluronic acid derivatives in various ratios (Shu et al., 2003, 2006). We have made extensive use of these hydrogels because their biochemical and biophysical characteristics can be optimized for a given cell type, or mixtures of several cell types, by adding additional proteins or cross-linkable heparin to mimic the role of heparan sulfate proteoglycans (Riley

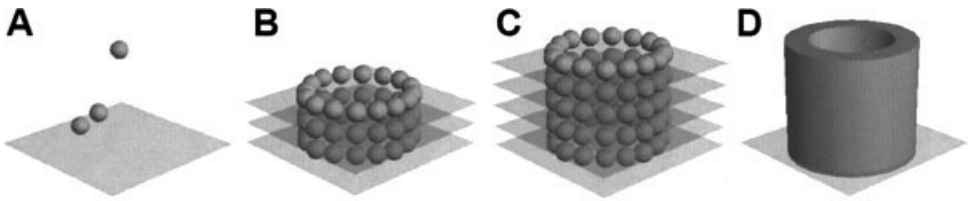

Figure 3. The stepwise process of printing. **A:** First, a layer of biocompatible hydrogel (bio-paper) is printed. **B:** Then bio-ink droplets are deposited according to a predefined pattern (e.g., along circle if the desired construct is a tube). **C:** These steps are repeated along the vertical direction until the planned size is achieved. **D:** Within a few days the bio-ink particles fuse and the bio-paper is removed.

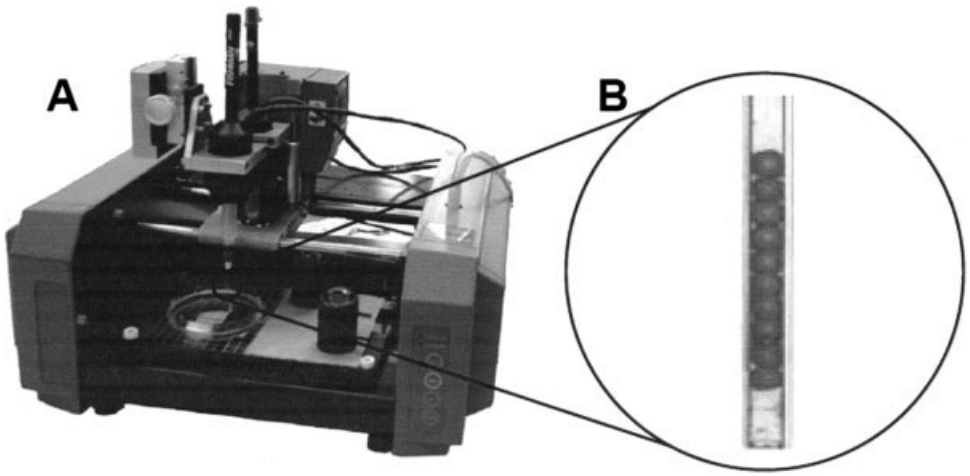

Figure 4. A: A twin-head bioprinter. One print head extrudes the bio-paper, the other delivers the bio-ink droplets one-by-one. **B:** A detailed view of the bioprinter's cartridge loaded with 500 μm diameter bio-ink droplets.

et al., 2006). As will be discussed later, the properties of the bio-paper intervene in several aspects in bioprinting.

The porous scaffolds used in classical TE and the bio-paper employed in the novel technology both represent biodegradable supportive structures for the engineered tissue. However they also differ in several respects. The bio-paper is printed concomitantly with the aggregates (see below), whereas scaffolds are preformed and subsequently seeded with cells. The bio-paper embeds the contiguous multicellular bio-ink particles, whereas scaffolds provide anchoring sites for individual cells. Once postprinting fusion of the bio-ink particles is complete and the stand-alone cellular structure has formed, the bio-paper is eliminated (it is not needed anymore). Scaffolds on the other hand are not separable from the cells that reside in them. They degrade upon implantation (together with the cells) into the host organism.

Printing

Figure 3 shows the principle of 3D tissue bioprinting. The process involves the computer-controlled, layer-by-layer deposition of hydrogels and spheroids of living cells. After depositing a layer of hydrogel in sol state, the aggregates are embedded into it one by one (Fig. 3A) while the sol-gel transition progresses due to change in pH or temperature. The process is repeated until the desired shape is obtained (Fig. 3B and C). The contiguous bio-ink droplets fuse and the bio-paper is eliminated by chemical (enzymes added), physical (temperature change), or biological means (enzymes secreted by cells) (Fig. 3D). The success of bioprinting hinges on the capability of the bio-paper to gel rapidly enough to maintain the aggregates in the specified configuration but slowly enough to allow continuity between successive layers.

The desktop bioprinter shown in Figure 4A is equipped with two print heads: one for hydrogel extrusion, the other for bio-ink particle delivery. Figure 4B shows a bio-ink cartridge: a glass micropipette loaded with cellular aggregates bathed in cell culture medium. Figure 5 shows some of the specific patterns printed with the printer (Jakab et al., 2004; Neagu et al, 2005). Computer scripts control the spatial deposition of the gel and aggregates.

The resolution of the printing device (Fig. 4A) itself is on the order of microns. The typical resolution of the bio-printed structures shown in Figure 5, on the other hand, depends on the diameter of the bio-ink particle (we typically use droplets of 300–500 μm). Smaller feature sizes may be attained by spontaneous postprinting rear-

rangements of the various cell types within the construct. The size of nonvascularized bio-printed structures in general is strongly limited by the ability of the nutrients to diffuse into the structure ($\sim$200 μm). (Note that this limitation, in principle, does not affect the size of the structures shown in Fig. 5; i.e., diameter of the rings and the lateral dimensions of the sheet). Limitations on the size of bio-printable structures will ultimately be disposed of when the vascularization of engineered tissues becomes possible.

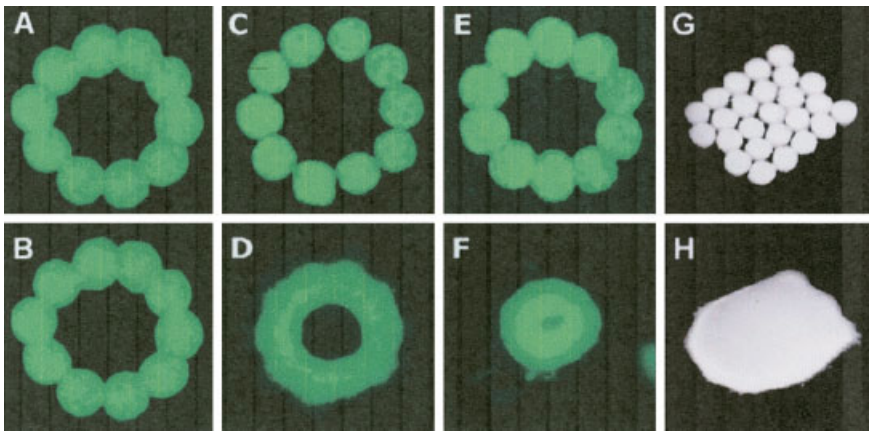

Figure 5. Initial (upper row) and final (lower row) configurations of toroidal structure (**A**–**F**) and cell sheet formation (**G**,**H**). The aggregates (500 μm in diameter) were embedded in agarose gels (A,B) and collagen gels at 1.0 mg/ml (C,D,G,H) and 1.7 mg/ml (E,F).

Postprocessing

Postprocessing refers to the postprinting incubation of the printed construct in a bioreactor, in the course of which adjacent bio-ink droplets fuse, giving rise to a connected structure able to resist mechanical stresses arising from manipulation and perfusion. Tube-like (Jakab et al., 2004) and sheet-like constructs (Neagu et al., 2005) have been printed in different gels as proof-of-concept studies. Figure 5 shows the initial and fused states after a week of incubation. It demonstrates that the composition of the bio-paper affects strongly the fusion process. It modulates the rate at which the bio-ink particles coalesce. It must provide the right spatial and temporal control over the release of growth factors. As it eventually needs to be eliminated, its removal rate, controlled by physical, chemical, or biological mechanisms, needs to be compatible with the maturation of the tissue construct.

Tissue engineered construct maturation, besides physiological temperatures, and gas and nutrient exchange, also requires tissue-specific mechanical conditioning. Cartilage, bone, ligament, cardiac tissues, blood vessels, and heart valves require specific mechanical stresses and strains to improve their mechanical properties. Therefore, a variety of bioreactors have been developed that aim at providing specific biomimetic conditions for the engineered construct (Vunjak-Novakovic, 2003; Martin et al., 2004; Martin and Vermette, 2005; Bilodeau and Mantovani, 2006).

With the development of scaffold-free techniques, like the one presented here, new challenges arise also for bioreactor design. For example, a bioprinted vascular tube will initially require a very gentle laminar flow of medium, similar to the one produced in the HARV. This will allow the fusion to occur and the 3D structure to shape. Later on, a biomimetic pulsatile perfusion flow will be necessary to assure proper cell growth, mechanical properties, and cellular composition (by the appropriate conditioning of endothelial cells).

Postprinting structure maturation is a complex process that depends on many factors, whose relative importance is hard to assess. Thus most TE efforts at present are of ''trial and error'' type. To make progress, in our tissue-liquidity–based approach we resort to computer simulations.

COMPUTER SIMULATIONS OF POSTPRINTING TISSUE REMODELING

According to DAH, tissue patterning results from such rearrangements of cells that progressively lower the total energy of adhesion between cells, or between cells and the ECM (Steinberg, 1963, 1996). Early computer simulations based on the DAH were confined to two dimensions and relied on deterministic cell motility rules (Leith and Goel, 1971). More recently, a stochastic motility rule implemented by the Metropolis algorithm (Metropolis et al., 1953), applied to the ''cellular'' version of the Potts model (familiar from statistical physics), proved effective in simulating tissue liquidity by the Monte Carlo method. In particular, the Potts model was employed to simulate cell sorting and the mutual engulfment of adjacent tissue fragments (Graner and Glazier, 1992; Glazier and Graner, 1993).

Inspired by the approach of Glazier and Graner (1993), we have constructed a 3D lattice model aimed at meeting practical TE needs, suitable for simulations of cellular self-assembly in systems of about 10^6 interacting cells (Jakab et al., 2004; Neagu et al., 2005). The sites of the cubic lattice are occupied by either (model) cells or similar-sized volume elements of the embedding medium (cell culture medium or a hydrogel). Site occupancy is specified by an integer, the cell type index σ. The interaction of adjacent particles of types σ and σ' is expressed via the mechanical works, $\varepsilon_{\sigma\sigma'}$, needed to separate them. The mechanical works are positive quantities known in the theory of liquids as work of cohesion for $\sigma = \sigma'$ or

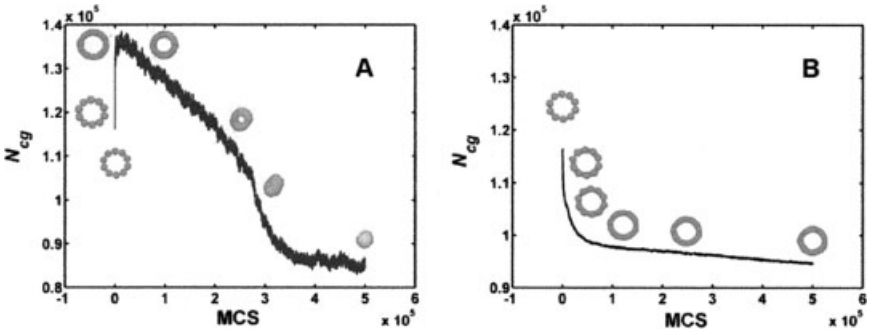

Figure 6. Simulated evolution of the tissue–medium interfacial area during multicellular aggregate fusion in a toroidal configuration, as measured by the number of cell–gel bonds, N_{cg}. Snapshots of model tissue conformations are depicted along the plot. The initial state consists of 10 aggregates, of 4169 cells each, placed along a circle at an average distance of two lattice spacings (i.e., distance between lattice sites) between their adjacent surfaces. The left panel (**A**) describes a simulation of 0.5×10^6 MCS with a relatively low interfacial tension ($\gamma_{cg} = 0.3E_T$). A similar simulation, but with a larger interfacial tension parameter, $\gamma_{cg} = 0.7E_T$, leads to a long-lived, ring-like structure (**B**).

work of adhesion for $\sigma \neq \sigma'$ (Israelachvili, 1992).

The total interaction energy of the model tissue is written as

$$E = \sum_{\langle r,r' \rangle} J(\sigma_r, \sigma_{r'}), \qquad (1)$$

where r and r' label lattice sites and $\langle r,r' \rangle$ stands for summation over close (nearest, next-nearest, and second-nearest) neighbors. The contact interaction energies $J(\sigma_r,\sigma_{r'})$ in Eq. [1] are expressed in terms of the works of cohesion/adhesion, $\varepsilon_{\sigma\sigma'}$. For example, in the case of a single cell type surrounded by medium, $J(\sigma_r,\sigma_{r'})$ may take one of the values $J(1,1) = -\varepsilon_{11}$, $J(2,2) = -\varepsilon_{22}$, and $J(1,2) = J(2,1) = -\varepsilon_{12}$, where $\sigma = 1$ stands for medium and $\sigma = 2$ refers to cells. (The inclusion of the negative sign in the Js is due to historical reasons.) Morphogenesis is achieved by reshaping interfacial boundaries between distinct cell populations (i.e., compartments). Similarly, in our model system evolution is driven by interfacial rearrangements. Identifying interfacial contributions to the sum from the right hand side of Eq. [1], the interaction energy of a system composed of T types of particles may be recast in the form (Neagu et al., 2006):

$$E = \sum_{\substack{\sigma,\sigma'=1 \\ \sigma<\sigma'}}^{T} \gamma_{\sigma\sigma'} \cdot N_{\sigma\sigma'} + \text{const.} \qquad (2)$$

Here $N_{\sigma\sigma'}$ is the number of bonds between particles of type σ and type $\sigma' \neq \sigma$. The second term on the right hand side of Eq. [2] denotes the constant contribution of the bulk. (As the cellular system evolves, the only quantity that varies is $N_{\sigma\sigma'}$). Since the energetically driven rearrangements of the system involve only energy differences, dropping the constant in Eq. [2] has no consequences. Thus, evolution is governed by the interfacial tension parameters, which are specific combinations of the interaction energies (Jakab et al., 2004):

$$\gamma_{\sigma\sigma'} = \frac{1}{2}(\varepsilon_{\sigma\sigma} + \varepsilon_{\sigma'\sigma'}) - \varepsilon_{\sigma\sigma'}. \qquad (3)$$

The computational algorithm used to simulate the self-assembly of cells into tissues is a special case of the Metropolis algorithm (Metropolis et al., 1953). The lattice representation of the initial state is constructed in accordance with the experimental protocol used to prepare the tissue construct (i.e., to accurately deliver the multicellular bio-ink particles into the bio-paper). First, cells located on interfaces (i.e., either between two aggregates or between an aggregate and the bio-paper) are identified. Next, within one Monte Carlo step (MCS), each interfacial cell (in random order) performs one trial move that consists in swapping positions with a randomly selected particle of different type. The move is accepted with a probability $P = \min(1,\exp(-\Delta E/E_T))$, where ΔE is the corresponding change in energy. This amounts to accepting each energy-lowering move with probability = 1, and moves that raise the energy with smaller probability. We adopted fixed boundary conditions to represent the experimental condition that cell movement is confined to the region occupied by medium.

The acceptance probability includes the biological fluctuation energy, E_T, a measure of cell motility. Note that the intimate mechanisms of movements in liquids are fundamentally different from those observed in cellular systems: liquid molecules move primarily due to their thermal energy, with scale set by k_BT (k_B, Boltzmann's constant; T, absolute temperature), whereas cell motility is powered by metabolic energy, with scale, E_T, set by ATP hydrolysis and manifested in cytoskeletally-driven membrane rufflings (Mombach and Glazier, 1996); E_T has been assessed for certain embryonic cell types (Beysens et al., 2000). The tissue-liquid analogy suggests a correspondence between the two energy scales. In our model, works of adhesion/cohesion and interfacial tension parameters are all expressed in units of E_T.

The simulation of aggregate fusion by the above-described Monte Carlo method is shown in Figure 1. A simulation of postprinting self-assembly of model cells into a tube-like or toroidal structure is described in Figure 6. The solid curves represent the interfacial area (i.e., the number of cell-gel bonds) versus the number of elapsed MCS with snapshots of typical intermediate conformations, shown along the curve. Figure 6A

corresponds to the case of a low cell-medium (i.e., cell–gel) interfacial tension parameter ($\gamma_{12} = 0.3E_T$). The initial increase of the cell–gel interfacial area is due to fluctuation-driven deviations of the aggregates from the spherical shape and to cell migration into the embedding hydrogel; once the torus emerges, it starts to shrink, thereby reducing the tissue-gel interfacial area, and finally rounding into a single spheroid. This scenario is similar to that observed in 1.7 mg/ml collagen gels (Fig. 5E and F). On the other hand, if the interfacial tension parameter γ_{12} is sufficiently large ($0.7E_T$ in the simulation in Fig. 6B), the toroidal conformation is similar to a metastable state: its evolution is slow enough to allow for the manipulation of the tissue construct and for its transfer into specialized bioreactors for maturation. Such a behavior was observed experimentally in 1 mg/ml collagen gels (Fig. 5C and D).

As illustrated in Figure 6A, sudden changes in the slope of the graph of the interfacial area versus MCS are signatures of topological changes of the model tissue construct. For example, the jump in the slope in Figure 6A at 270×10^3 MCS corresponds to the moment when the doubly connected torus turns into a simply connected, pancake-shaped structure.

In principle, the conclusions drawn from simulations of a toroidal geometry are expected to remain valid also for tubular structures built from several superimposed rings of aggregates since fusion will take place also between rings.

DISCUSSION AND CONCLUSIONS

We described a novel TE approach to build 3D living structures that differs from classical approaches both in its scientific foundation and technology. The approach relies on tested principles of developmental biology, specifically tissue liquidity. It employs tissue liquidity by operating with multicellular spherical aggregates that upon contact fuse. Fusion is implemented through bioprinting (the technological novelty of the method), the automated, spatially accurate delivery of the bio-ink aggregates into the 3D environment, the bio-paper.

Compared to scaffold-based TE and the emerging other rapid prototyping techniques (RP) (Boland et al., 2006; Smith et al., 2007), our method offers several advantages. Printing aggregates as opposed to individual cells assures significant gain in speed. It also allows achieving higher cell densities than in methods that use cellular solutions (Boland et al., 2006) or the seeding of cells into porous scaffolds (Vunjak-Novakovic et al., 1998). Although bioprinting utilizes ECM-like materials (i.e., hydrogels), their role here strongly differs from that in scaffolds. The bio-paper is employed to allow the bio-ink particles to flow and thus bring about the postprinting structure. As long as it allows cells to move, even if it is not fully biocompatible, it does not necessarily prevent structure formation, as its contact with the cells is constrained both in space (only through cells located on the surface of each bio-ink droplet) and time (only from the initiation of printing until fusion has sufficiently progressed). Therefore, one may also use hydrogels in which the phase transition from a liquid to a swollen network is induced by conditions such as changes of pH or temperature that may otherwise be harsh for cells. This is not the case in the RP, in which a cell suspension is mixed with the hydrogel solution before deposition (Boland et al., 2006; Smith et al., 2007).

Among the present limitations of the bioprinting method outlined here we mention the need of a large number of cells for bio-ink preparation, the difficulties related to large-scale production, manipulation and maintenance of bio-ink droplets, the need for the precise timing of the sol-gel transition in the bio-paper, and the mechanical sensitivity of the printed construct until fusion is completed. Hopefully these limitations will be overcome in the near future, offering a new way to respond to the rapidly growing demand for replacement organs.

ACKNOWLEDGMENTS

Computational resources provided by the University of Missouri Bioinformatics Consortium (UMBC) are acknowledged.

REFERENCES

Beysens DA, Forgacs G, Glazier JA. 2000. Cell sorting is analogous to phase ordering in fluids. Proc Natl Acad Sci USA 97:9467–9471.

Bilodeau K, Mantovani D. 2006. Bioreactors for tissue engineering: focus on mechanical constraints. A comparative review. Tissue Eng 12:2367–2383.

Boland T, Xu T, Damon B, Cui X. 2006. Application of inkjet printing to tissue engineering. Biotechnol J 1:910–917.

Callebaut M, Van Nueten E, Border H, Harrisson F. 2004. Induction of the avian coelom with associated vitelline blood circulation by Rauber's sickle derived junctional endoblast and its fundamental role in heart formation. J Morphol 259:21–32.

Chen HC. 2006. Bioreactors for tissue engineering. Biotechnol Lett 28:1415–1423.

Colas JF, Schoenwolf GC. 2001. Towards a cellular and molecular understanding of neurulation. Dev Dyn 221:117–145.

Flenner E, Marga F, Neagu A, et al. 2007. Relating biophysical properties across scales. Curr Top Dev Biol 81:461–483.

Forgacs G, Foty RA, Shafrir Y, Steinberg MS. 1998. Viscoelastic properties of living embryonic tissues: a quantitative study. Biophys J 74: 2227–2234.

Foty RA, Forgacs G, Pfleger CM, Steinberg MS. 1994. Liquid properties of embryonic tissues. Measurement of interfacial tensions. Phys Rev Lett 72:2298–2301.

Foty RA, Pfleger CM, Forgacs G, Steinberg MS. 1996. Surface tensions of embryonic tissues predict their mutual envelopment behavior. Development 122:1611–1620.

Foty RA, Steinberg MS. 2005. The differential adhesion hypothesis: a direct evaluation. Dev Biol 278:255–263.

Frenkel J. 1945. Viscous flow of crystalline bodies under the action of surface tension. J Phys (USSR) 9:385–391.

Glazier JA, Graner F. 1993. Simulation of the differential adhesion driven rearrangement of biological cells. Phys Rev E 47:2128–2154.

Godt D, Tepass U. 1998. Drosophila oocyte localization is mediated by differential cadherin-based adhesion. Nature 395:387–391.

Gonzalez-Reyes A, St Johnston D. 1998. The Drosophila AP axis is polarised by the cadherin-mediated positioning of the oocyte. Development 125:3635–3644.

Gordon R, Goel NS, Steinberg MS, Wiseman LL. 1972. A rheological mechanism sufficient to explain the kinetics of cell sorting. J Theor Biol 37:43–73.
Graner F, Glazier JA. 1992. Simulation of biological cell sorting using a 2-dimensional extended Potts-model. Phys Rev Lett 69:2013–2016.
Griffith LG, Naughton G. 2002. Tissue engineering-current challenges and expanding opportunities. Science 295: 1009–1014.
Hayashi T, Carthew RW. 2004. Surface mechanics mediate pattern formation in the developing retina. Nature 431:647–652.
Hegedus B, Marga F, Jakab K, et al. 2006. The interplay of cell-cell and cell-matrix interactions in the invasive properties of brain tumors. Biophys J 91:2708–2716.
Heid PJ, Raich WB, Smith R, et al. 2001. The zinc finger protein DIE-1 is required for late events during epithelial cell rearrangement in *C-elegans*. Dev Biol 236:165–180.
Hollister SJ. 2005. Porous scaffold design for tissue engineering. Nat Mater 4:518–524.
Hubbell JA. 1996. Hydrogel systems for barriers and local drug delivery in the control of wound healing. J Control Release 39:305–313.
Israelachvili J. 1997. Intermolecular and surface forces. New York: Academic Press. p. 313.
Jakab K, Neagu A, Mironov V, et al. 2004. Engineering biological structures of prescribed shape using self-assembling multicellular systems. Proc Natl Acad Sci USA 101:2864–2869.
Jakab K, Damon B, Neagu A, et al. 2006. Three-dimensional tissue constructs built by bioprinting. Biorheology 43:509–513.
Langer R, Vacanti JP. 1993. Tissue engineering. Science 260:920–926.
Lay Flurrie K. 2004. The properties of hydrogel dressings and their impact on wound healing. Prof Nurse 19: 269–273.
Lecuit T, Lenne P-F. 2007. Cell surface mechanics and the control of cell shape, tissue patterns and morphogenesis. Nat Rev Mol Cell Biol 8:633–644.
Lee KY, Mooney DJ. 2001. Hydrogels for tissue engineering. Chem Rev 101:1869–1880.
Leith AG, Goel NS. 1971. Simulation of movement of cells during self-sorting. J Theor Biol 33:171–188.
Martin I, Wendt D, Heberer M. 2004. The role of bioreactors in tissue engineering. Trends Biotechnol 22:80–86.
Martin Y, Vermette P. 2005. Bioreactors for tissue mass culture: Design, characterization, and recent advances. Biomaterials 26:7481–7503.
Metropolis N, Rosenbluth AW, Rosenbluth MN, Teller AH, Teller E. 1953. Equation of state calculations by fast computing machines. J Chem Phys 21:1087–1097.
Mombach JCM, Glazier JA. 1996. Single cell motion in aggregates of embryonic cells. Phys Rev Lett 76:3032–3035.
Mooney D, Hansen L, Vacanti J, et al. 1992. Switching from differentiation to growth in hepatocytes: control by extracellular matrix. J Cell Physiol 151:497–505.
Munoz-Chapuli R, Carmona R, Guadix JA, et al. 2005. The origin of the endothelial cells: an evo-devo approach for the invertebrate/vertebrate transition of the circulatory system. Evol Dev 7:351–358.
Neagu A, Jakab K, Jamison R, Forgacs G. 2005. Role of physical mechanisms in biological self-organization. Phys Rev Lett 95:178104.
Neagu A, Kosztin I, Jakab K, et al. 2006. Computational modeling of tissue self-assembly. Mod Phys Lett B 20:1217–1231.
Papenfuss EJ. 1934. Reunition of pieces in Hydra, with special reference to the role of three layers and to the fate of differentiated parts. Biol Bull 67:223–243.
Perez-Pomares JM, Munoz-Chapuli R. 2002. Epithelial-mesenchymal transitions: a mesodermal cell strategy for evolutive innovation in Metazoans. Anat Rec 268:343–351.
Perez-Pomares JM, Foty RA. 2006. Tissue fusion and cell sorting in embryonic development and disease: biomedical implications. Bioessays 28: 809–821.
Prestwich GD. 2007. Simplifying the extracellular matrix for 3-D cell culture and tissue engineering: a pragmatic approach. J Cell Biochem 101:1370–1383.
Prewett T, Goodwin T, Spaulding G. 1993. Three-dimensional modeling of T-24 human bladder carcinoma cell line: A new simulated microgravity culture vessel. J Tissue Cult Methods 15:29–36.
Riley CM, Fuegy PW, Firpo MA, et al. 2006. Stimulation of in vivo angiogenesis using dual growth factor-loaded crosslinked glycosaminoglycan hydrogels. Biomaterials 27:5935–5943.
Shu XZ, Liu Y, Palumbo F, Prestwich GD. 2003. Disulfide-crosslinked hyaluronan-gelatin hydrogel films: a covalent mimic of the extracellular matrix for in vitro cell growth. Biomaterials 24:3825–3834.
Shu XZ, Ahmad S, Liu Y, Prestwich GD. 2006. Synthesis and evaluation of injectable, in situ crosslinkable synthetic extracellular matrices for tissue engineering. J Biomed Mater Res A 79A:902–912.
Silva EA, Mooney DJ, Gerald PS. 2004. Synthetic extracellular matrices for tissue engineering and regeneration. Curr Top Dev Biol 64:181–205.
Smith CM, Christian JJ, Warren WL, Williams SK. 2007. Characterizing environmental factors that impact the viability of tissue-engineered constructs fabricated by a direct-write bioassembly tool. Tissue Eng 13:373–383.
Steinberg MS. 1963. Reconstruction of tissues by dissociated cells. Some morphogenetic tissue movements and the sorting out of embryonic cells may have a common explanation. Science 141:401–408.
Steinberg MS. 1970. Does differential adhesion govern self-assembly processes in histogenesis? Equilibrium configurations and the emergence of a hierarchy among populations of embryonic cells. J Exp Zool 173:395–434.
Steinberg MS, Poole TJ. 1982. Liquid behavior of embryonic tissues. In: Bellairs R, Curtis ASG, Dunn G, editors. Cell behaviour. Cambridge: Cambridge University Press. pp 583–607.
Steinberg MS. 1996. Adhesion in development: an historical overview. Dev Biol 180:377–388.
Technau U, Holstein TW. 1992. Cell sorting during the regeneration of Hydra from reaggregated cells. Dev Biol 151:117–127.
Vacanti JP, Langer R. 1999. Tissue engineering: the design and fabrication of living replacement devices for surgical reconstruction and transplantation. Lancet 354(Suppl 1):32–34.
Vunjak-Novakovic G, Obradovic B, Martin I, et al. 1998. Dynamic cell seeding of polymer scaffolds for cartilage tissue engineering. Biotechnol Prog 14:193–202.
Vunjak-Novakovic G. 2003. The fundamentals of tissue engineering: scaffolds and bioreactors. In: Tissue engineering of cartilage and bone. Novartis Foundation Symposia. Novartis Foundation. New York: John Wiley & Sons. pp 34–51.
Wang X, Wei G, Yu W, et al. 2006. Scalable producing embryoid bodies by rotary cell culture system and constructing engineered cardiac tissue with ES-derived cardiomyocytes in vitro. Biotechnol Prog 22:811–818.
Wessels A, Sedmera D. 2003. Developmental anatomy of the heart: a tale of mice and man. Physiol Genomics 15:165–176.
Whitesides GM, Boncheva M. 2002. Supramolecular chemistry and self-assembly special feature: beyond molecules: self-assembly of mesoscopic and macroscopic components. Proc Natl Acad Sci USA 99:4769–4774.
Williams-Masson EM, Malik AN, Hardin J. 1997. An actin-mediated two-step mechanism is required for ventral enclosure of the *C. elegans* hypodermis. Development 124:2889–2901.
Wilson H. 1907. A new method by which sponges may be artificially reared. Science 25:912–915.